International Journal of Applied Pharmaceutics

ISSN- 0975-7058 Vol 14, Issue 5, 2022

Original Article

DEVELOPMENT AND OPTIMIZATION OF ASTRAGALIN-LOADED POLYMERIC NANOPARTICLES USING CENTRAL COMPOSITE FACTORIAL DESIGN

S. KALIDAS[1], P. GEETHA[2*]

[1,2]Vels Institute of Science, Technology and Advanced Studies (VISTAS), School of Pharmaceutical Sciences, Chennai 600117, India
*Email: lgeethapharma.sps@velsuniv.ac.in

Received: 03 Feb 2022, Revised and Accepted: 22 Jun 2022

ABSTRACT

Objective: The objective of the present study was to develop and optimize Astragalin-loaded polymeric nanoparticles (AST-NPs) using a central composite factorial design (CCD).

Methods: AST-NPs were prepared by the dialysis method. CCD was employed to study the influence of formulation factors, polymer concentration, aqueous organic phase ratio, and process parameter stirring time on dependent physicochemical characteristics, particle size, zeta potential, and percentage entrapment efficiency (%EE) of the drugs. The optimized formulation was evaluated for *in vitro* release studies and subjected to stability studies.

Results: Polymer concentration and process parameters were optimized to produce nanoparticles with desired parameters. The prepared NPs were characterized by Fourier transmission infrared (FT-IR), differential scanning calorimetry (DSC), drug loading, entrapment efficiency, particle size, zeta potential, and *in vitro* studies. FT-IR and DSC studies indicated that there was no interaction between the drug and polymer. The optimized NPs exhibits stability. Optimized NPs exhibited spherical and porous surfaces with a mean PS of 118 nm, the zeta potential of-25 mV, and %EE of 89%.

Conclusion: Astragalin-loaded nanoparticles prepared with optimized formulation composition and process parameters.

Keywords: Polymeric nanoparticles, Central composite factorial design, *In vitro* release, Percentage entrapment efficiency

DOI: https://dx.doi.org/10.22159/ijap.2022v14i5.44315. Journal homepage: https://innovareacademics.in/journals/index.php/ijap

INTRODUCTION

Medicinal plants have been an infinite source of therapeutic agents for millions of years. Most of the discovered drugs belong to natural products are derivatives of natural compounds [1, 2]. A lot of plant-derived bioactive compounds are used for the cure as well as for the prevention of several diseases. Among these compounds are the polyphenols consisting of alcohols with ≥2 benzene rings and ≥1 hydroxyl group. These polyphenols have a range from simple structural molecules (flavonoids and phenylpropanoids) to highly complex compounds (lignins and melanins). Reports have suggested that polyphenols in general and flavonoids in particular exhibit various biological effects like antiallergic, antibacterial, anti-inflammatory, antiviral, antithrombic, hepatoprotective, antibacterial, and antioxidant activities [2, 3]. Astragalin (kaempferol-3-O-β-D-glucoside), a bioactive natural flavonoid, has been well known for its medicinal importance. It has been reported to exhibit multiple pharmacological properties including antioxidant [3, 4], anti-inflammatory [5], anticancer [6], neuroprotective [7], and cardioprotective properties [7].

Nanotechnology is rapidly expanding in the food and pharmaceutical industries [8, 9]. One of the main applications of nanotechnology is the nano-encapsulation of bioactive compounds for biological purposes. During the nano-encapsulation process, besides bioactive protection, their bioavailability also is improved due to an increase in the surface-to-volume ratio by reducing particle size into the nano-range [10].

Nanoparticles are defined as sub-micron solid particles, which can be used for nano-encapsulation of bioactive compounds [11]. Depending upon the method of preparation, nanoparticles, nano-spheres or nano-capsules can be obtained. Nano-spheres are matrix systems in which the bioactive compounds are physically and uniformly dispersed, while nano-capsules are vesicular systems in which the bioactive compounds are confined to a cavity consisting of an inner liquid core surrounded by a polymeric membrane. Biodegradable polymeric nanoparticles can be produced from proteins (such as gelatin and milk proteins), polysaccharides (such as chitosan, sodium alginate, and starch), and synthetic polymers (such as poly (d,l-lactide), poly (lactic acid) PLA, poly (d,l-glycolide), PLG, poly (lactide-co-glycolide), PLGA, and poly (cyanoacrylate) PCA) [12].

The dispersion of preformed polymers and the polymerization of monomers are generally the two main strategies for the preparation of polymeric nanoparticles. However, there are various methods used for the preparation of polymeric nanoparticles such as desolvation, dialysis, ionic gelation, nanoprecipitation, solvent evaporation, salting out, spray drying, and supercritical fluid [12].

In the present study, Astragalin-loaded polymeric nanoparticles were prepared by the dialysis method.

MATERIALS AND METHODS

Materials

Astragal in and Polylactic acid (PLA) were purchased from Merck Sigma-Aldrich India, Dimethyl sulfoxide (DMSO), and all other HPLC grade solvents were obtained from Thermo Scientific, India.

Preparation of Polymeric nanoparticles

The astragal in-loaded nanoparticles were prepared by a dialysis method [13]. Astragal in (5 mg) and PLA (50 mg) were dissolved in DMSO (1 ml) and added dropwise to 25 ml of water under stirring. The mixture was stirred for another 30 min at room temperature and dialyzed against distilled water using a 7 kDa dialysis bag for 24 h. The unentrapped astragal in was removed by filtration through a 0.45 µm filter and freeze-dried.

Drug loading and encapsulation efficiency

The following equations were used to calculate the DL efficiency and encapsulation efficiency (EE). The concentration of astragalin was detected by high-performance liquid chromatography (HPLC) system using a C18 column (5 µm, 4.6×250 mm). The mobile phase consisted of a mixture of methyl alcohol, water, and acetonitrile (23:41:36, v/v) delivered at a flow rate of 1.0 ml/min. The injection volume was 20 µl and the wavelength was set at 227 nm.

$$DL = \frac{\text{Amount of AST in NPs}}{\text{Amount of AST} - \text{Loaded NPs}} \times 100$$

$$EE = \frac{\text{Amount of AST in NPs}}{\text{Amount of AST for loading}} \times 100$$

Experimental design

Initial experiments showed that the variables, such as polymer concentration, stirring time, and also the proportion of aqueous to organic phase throughout preparation work, were the major variables that influenced the particle size, zeta potential as well as encapsulation efficiency of the astragalin polymeric nanoparticles. Hence, a central composite rotatable design-response surface methodology (CCRD-RSM) was made used to systemically examine the impact of these 3 important formulation variables on particle size, zeta potential as well as encapsulation efficiency of the prepared astragalin polymeric nanoparticles [14, 15]. For every element, the speculative range was picked based on the outcomes of initial experiments and also the feasibility of preparing the astragalin polymeric nanoparticles at extreme values. The value range of the variables was polymer concentration (X1) of 1–50 mg/ml, stirring time (X2) of 1-60 min, and also the proportion of aqueous to organic phase (X3) of 15:1. A total amount of 20 examinations were performed. All the formulations in these experiments were prepared in replicate.

Table 1: The variables and their level studied in the experiment

Independent variables	Levels		
	-1	0	+1
Polymer concentration	1	27.50	50
Stirring time	1	37.50	60
Aqueous to organic phase ratio	1	10.00	15

Characterization of nanoparticle

Measurement of particle size

The average particle size (*z*-average) and polydispersity index (PDI) of the developed nanoparticles were determined by laser dynamic light scattering using Malvern Zetasizer (Malvern, Worcestershire, UK). Particle size investigation was performed in triplicate by diluting NPs suspension to 1/50 v/v in HPLC water.

The PDI value indicates the particle size distribution of nanoparticles in a given sample. The higher value of PDI indicates the distribution of NPs with variable size range, which results in the formation of aggregates and could result in low stability of particle suspension and low homogeneity.

Zeta potential

The nanoparticles suspension was diluted fifty times with HPLC water and zeta potential was measured using Malvern Zetasizer (Malvern, Worcestershire, UK). Zeta potential indicates the surface charge on the particles and was measured to determine the stability of nanoparticles in the suspension.

Scanning electron microscopy (SEM) measurement

The samples for SEM were mounted on metal stubs, and the surface and surface morphology of the particles were examined by a Hitachi S4800 Field Emission SEM (Hitachi, Gaithersburg, MD, USA). The analytical parameters included an accelerating voltage of 10 KeV, a working distance of 13.5 mm, and a vacuum of 40 Pascals.

Differential scanning calorimetry (DSC) analysis

A DSC (Shimadzu DSC-60, Columbia, MD, USA) was used to analyze pure Astragalin, PLGA, and physical mixture and Astragalin NPs. The sample to be analyzed (3–5 mg) by DSC was crimped non-hermetically in an aluminum pan and heated from room temperature (23 °C) to 300 °C at a rate of 10 °C/min under nitrogen purge.

Fourier transform infrared (FTIR) analysis

FTIR analysis was performed to study the chemical interaction between drug and polymer using Perkin Elmer BX II (PerkinElmer, Massachusetts, USA). The samples were scanned in the IR range from 400 to 4000 cm^{-1}.

Encapsulation efficiency

The concentration of astragalin was detected by a high-performance liquid chromatography (HPLC) system using a C18 Luna column 5 m particle size, 25 cm × 3.00 mm I.D. (Phenomenex, Torrance, CA, USA). A mobile phase composed of water-formic acid (99.5:0.5, v/v) (solvent A) and acetonitrile (solvent B) was used. The flow rate was 0.5 ml/min. The injection volume was 10 L and the wavelength was set at 246 nm.

***In vitro* release study**

In vitro release of astragalin-loaded nanoparticles was evaluated by the dialysis bag diffusion technique. One hundred milliliters of phosphate buffer, pH adjusted to 7.4 were poured into a well-closed glass vessel as the dissolution medium for the *in vitro* release test. Astragalin NP (5 ml) was transferred to a dialysis bag (molecular weight cutoff 5000–10,000) and then the dialysis bag was placed in the glass vessel. The vessels were placed in an incubator shaker and shaken horizontally (Incubator Shaker ZHWY-200B, Shanghai Zhicheng Analysis Instrument Company, China) at 37 °C and 100 strokes per min. The sample (1 ml) was withdrawn from the system at predetermined time intervals and filtered through a 0.45 m hydrophilic filter membrane. The drug content was measured by the HPLC method described above. The diffusion profile of pure drug suspension through a dialysis bag was examined as a control. The pure drug suspension was prepared by dispersing 1 ml Astragalin solution (5 mg/ml) in 4 ml of double-distilled water. Each experiment was performed in triplicate.

Stability studies

Optimized AST-PLA-NPs were subjected to stability testing for six months as per ICH guideline at a temperature of 2-8 °C, 25±2 °C/60±5 % RH. Samples are stored in an amber-colored glass vial. The samples were analyzed for Particle size, Zeta potential, Assay, and drug release at a defined time interval.

Data analysis

The relationships between responses and formulation variables of all model formulations were treated by Design-Expert® software. Statistical analysis, including stepwise linear regression and response surface analysis was conducted. The significant terms (P<0.05) were chosen for the final equations. Suitable models consisting of three components include linear, quadratic, and special cubic models. The best-fitting mathematical model was selected based on the comparisons of several statistical parameters, including the coefficient of variation (c. v.), the multiple correlation coefficient (R^2), and the adjusted multiple correlation coefficient (adjusted R^2) proved by Design-Expert software. The significance of differences was evaluated using Student's *t*-test and one-way ANOVA at the probability level of 0.05.

RESULTS AND DISCUSSION

The CCRD–RSM constitutes an alternative approach because it offers the possibility of investigating a high number of variables at different levels with only a limited number of experiments. The variables in table 1 were picked considering our initial experiments. Table 2 revealed the speculative outcomes concerning the evaluated variables on drug encapsulation efficiency, mean particle size, and also zeta potential. The three dependent values varied from 68 to 94 % by weight, 153 to 210 nm, as well as-35 to 31 mV. A mathematical

relationship between factors and also parameters was produced by response surface regression evaluation making use of Design-Expert ® 11 software application. The three-dimensional (3D) response surface graphs for the most statistically significant variables on the evaluated parameters are displayed in fig. 1-3. The response surface diagram revealed that the mean particle size, zeta potential, and encapsulation efficiency were enhanced with an increase in polymer concentration. An increase in the stirring time and decrease in the polymer concentration decreases the particle size. As well, increasing in stirring time and an increase in polymer concentration increases the zeta potential. An increase in polymer concentration and aqueous to organic phase ratio increases the encapsulation efficiency. The optimized variables revealed an excellent fit to the second-order polynomial equation. After model simplification with backward elimination, the r-value decreased a little to 0.9545, 0.5866 as well as 0.7280, respectively. The lack of fit was not significant at a 95% self-confidence level. All the remaining parameters were significant at $p \leq 0.05$. The statistical analysis of the results produced the adhering to polynomial equations and is also provided in table 3. Anticipated optimum ranges of the independent variables are detailed in table 4. The fitting outcomes showed that the optimized nanoparticles with high entrapment efficiency, minimal particle size as well as ideal zeta potential was acquired with the polymer concentration of 50 mg/ml, stirring time of 60 min as well an aqueous to organic phase ratio of 5:1 v/v, respectively. Table 4 programs that the experimental values of both sets prepared within the optimum range were extremely near to the anticipated values, with low percent bias, recommending that the optimized formulation was trustworthy and also sensible. It can be ended that a high desirability value might be gotten with a polymer concentration of 50 mg/ml, stirring time of 60 min as well an aqueous to organic phase ratio of 5:1 v/v. The desirability acquired was 0.740 and also the same is represented in fig. 4. Perturbation plots exist in fig. 5-7 for anticipated models to get a much better understanding of the examined treatment. These sorts of plots reveal the impact of an independent factor on a particular response, with all various other aspects held consistent at a referral factor. A steepest incline or curvature suggests the sensitiveness of the response to a specific factor. Fig. 5 shows that stirring time had one of the most crucial impacts on particle size followed by polymer concentration and aqueous to organic phase ratio. Fig. 6 shows that stirring time had one of the most vital impacts on zeta potential, followed by polymer concentration and aqueous to organic phase ratio. Fig. 7 reveals that the aqueous to organic phase ratio had the most crucial result on encapsulation efficiency, followed by stirring time and polymer concentration.

Table 2: Central composite rotatable design generated by design expert 11® software along with the obtained response

Std	Run	Factor 1 A: polymer concentration mg/ml	Factor 2 B: stirring time min	Factor 3 C: Aqueous to organic phase ratio	Response 1 particle size nm	Response 2 zeta potential mV	Response 3 encapsulation efficiency %
18	1	27.5	37.5	10	210±6.1	-30±1.4	68±2.4
7	2	5	60	15	172±4.7	-31±1.8	78±3.6
8	3	50	60	15	176±5.2	-14±1.2	80±1.9
14	4	27.5	37.5	18.40	153±4.4	-24±2.1	94±2.1
15	5	27.5	37.5	10	210±3.7	-30±1.7	68±2.7
13	6	27.5	37.5	1.59	161±6.8	-35±1.9	82±2.5
19	7	27.5	37.5	10	210±4.9	-30±1.6	68±2.6
11	8	27.5	0.34	10	186±2.8	-28±1.6	79±1.7
6	9	50	15	15	159±7.5	-27±1.9	69±3.1
10	10	65.34	37.5	10	179±4.2	-33±2.6	86±2.4
20	11	27.5	37.5	10	210±7.5	-30±1.8	68±3.1
16	12	27.5	37.5	10	210±8.2	-30±2.4	68±3.6
1	13	5	15	5	183±5.4	9±1.6	84±1.7
3	14	5	60	5	177±8.3	16±1.5	78±1.4
12	15	27.5	75.34	10	166±5.6	10±1.4	91±1.3
17	16	27.5	37.5	10	210±4.9	-30±1.3	68±2.6
5	17	5	15	15	191±7.2	11±1.2	88±1.8
4	18	50	60	5	165±5.9	31±2.1	79±1.5
2	19	50	15	5	170±8.2	28±1.9	69±1.4
9	20	10.34	37.5	10	189±7.5	29±5	81±2.6

Data represent mean±SD, n = 3

Table 3: Reduced response models and statistical parameters obtained from ANOVA

Responses	Regression model	Adjusted R^2	Model P-value	%CV	Adequate precision
Particle size	PS=209.87-5.11A-3.41B-0.7655C+4.63AB-0.3750AC+1.13BC-8.33A2-11.16B^2-17.88C^2	0.8126	0.0001	3.28	21.28
Zeta potential	ZP=-30.50-6.68A+3.29B-9.26C+6.37AB-6.88AC-4.88BC+13.14A^2+10.67B^2 +3.42C^2	0.8563	0.0001	2.86	10.42
Encapsulation efficiency	EE=68.27-1.65A+1.84B+1.84C+4.62AB-0.3750AC-0.3750BC+3.70A^2+4.23B^2+5.29C^2	0.8824	0.0001	3.12	14.26
Acceptance criteria		1	<0.05	<4	>10

Table 4: Comparison of experimental and predicted values under optimal conditions for final formulation

Polymer concentration	Stirring time	Aqueous to organic phase ratio	Particle size	Zeta potential	Encapsulation efficiency
50 mg/ml	60 min	5:1			
Predicted			118	-24	90
Experimental			121±2.6	-25±1.4	89±2.1
Bias %			2.5%	4.1%	1.0%
Acceptance criteria 6%					
Bias was calculated as (predicted value-experimental value)/predicted value × 100					

Data represent mean±SD, n = 3

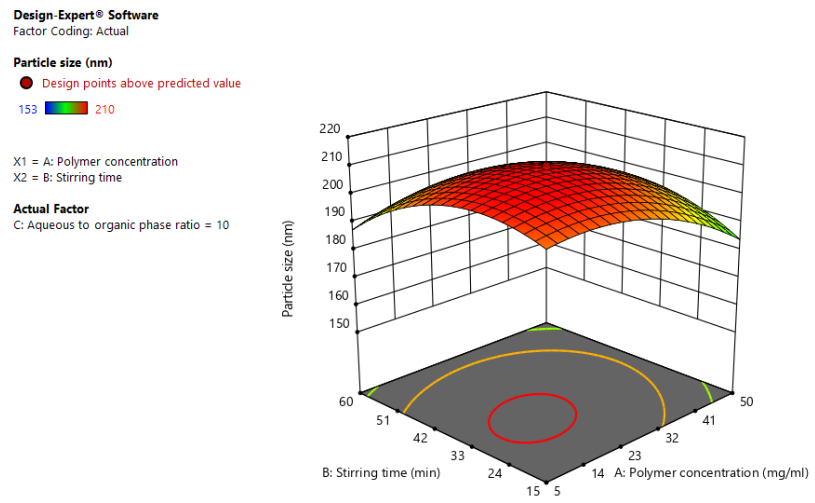

Fig. 1: Three-dimensional (3D) response surface plots showing the effect of the variable on response. The effect of polymer concentration and stirring time on particle size

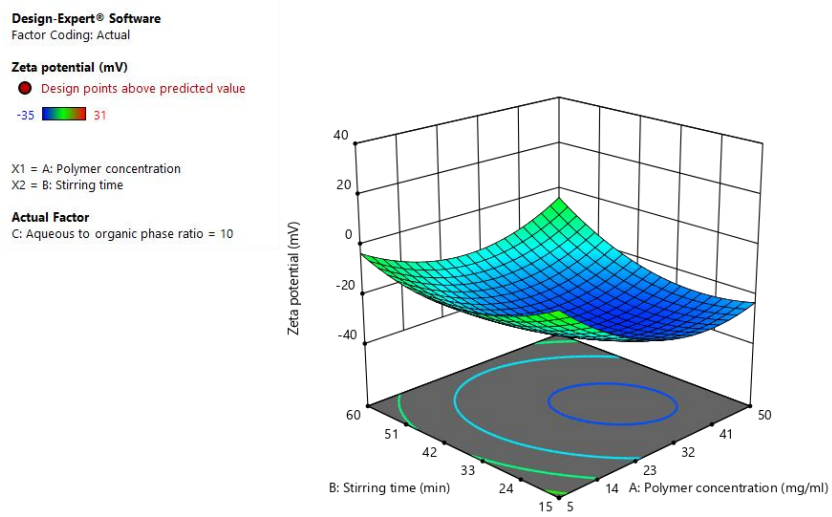

Fig. 2: Three-dimensional (3D) response surface plots showing the effect of the variable on response. The effect of polymer concentration and stirring time on zeta potential

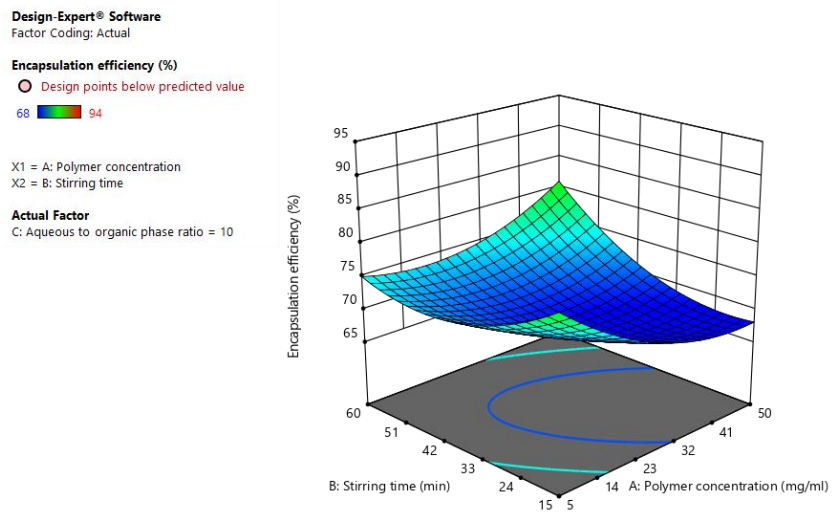

Fig. 3: Three-dimensional (3D) response surface plots showing the effect of the variable on response. The effect of polymer concentration and stirring time on the encapsulation efficiency

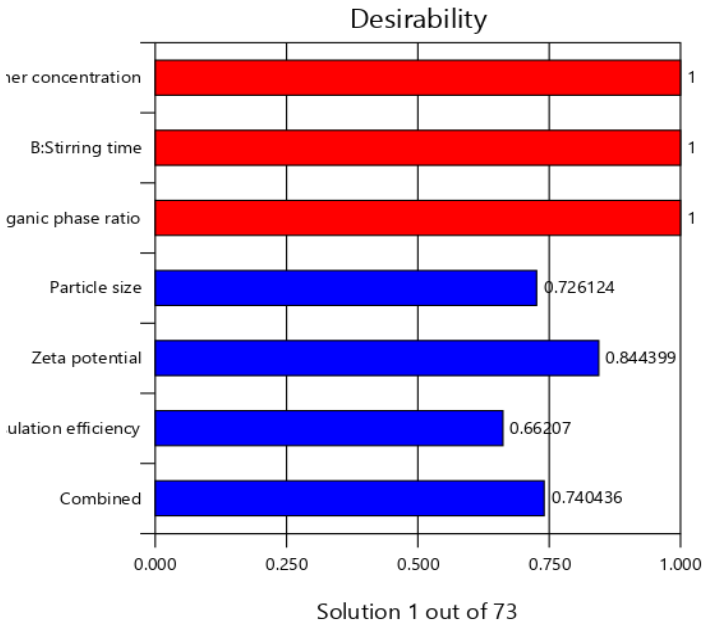

Fig. 4: Three-dimensional (3D) response surface plots showing the desirability with a value of 0.740

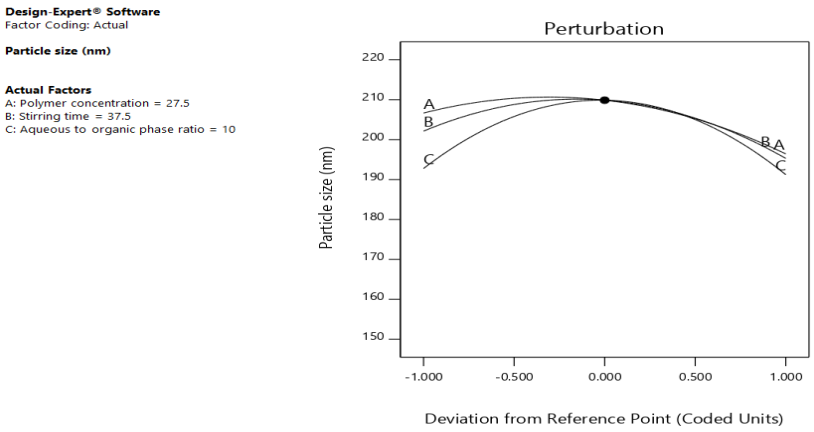

Fig. 5: Perturbation plot showing the effect of each of the independent variables on particle size where A, B, and C are polymer concentration, stirring time, and aqueous to organic phase ratio, respectively

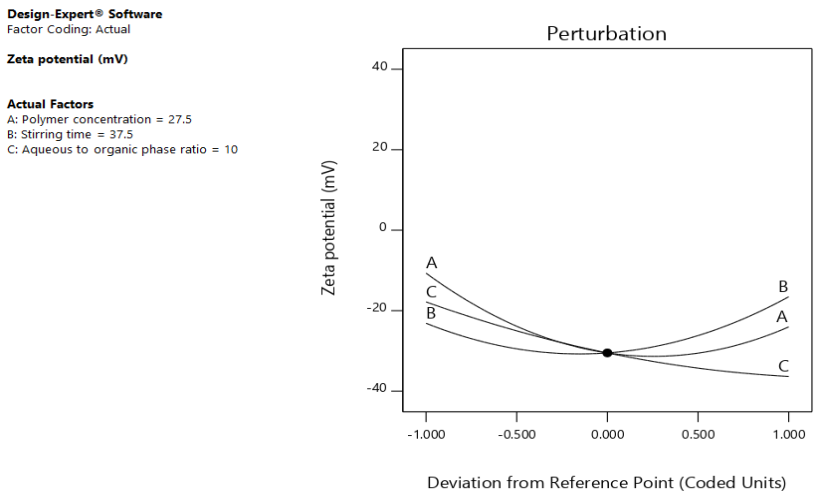

Fig. 6: Perturbation plot showing the effect of each of the independent variables on zeta potential where A, B, and C are polymer concentration, stirring time, and aqueous to organic phase ratio, respectively

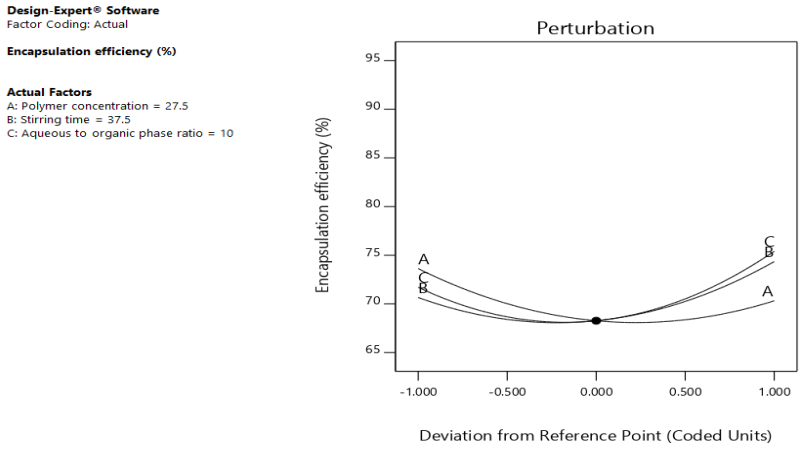

Fig. 7: Perturbation plot showing the effect of each of the independent variables on encapsulation efficiency where A, B, and C are polymer concentration, stirring time, and aqueous to organic phase ratio respectively

Particle size, zeta potential, and SEM measurement

The mean particle size of astragalin-loaded polymeric nanoparticles was 121±2.6 nm (fig. 8). The zeta potential of the same was found to be-25±1.4 mV (fig. 9), and it is sufficiently high to form stable pharmaceutical preparation. It is reported that nanoparticles with a large negative or positive value of zeta potential are less prone to aggregation or an increase in particle size indicate good stability [16]. To provide information on the morphology of the optimal astragalin-loaded polymeric nanoparticles, SEM was used to take photos, as shown in fig. 10. The optimized nanoparticles are spherical.

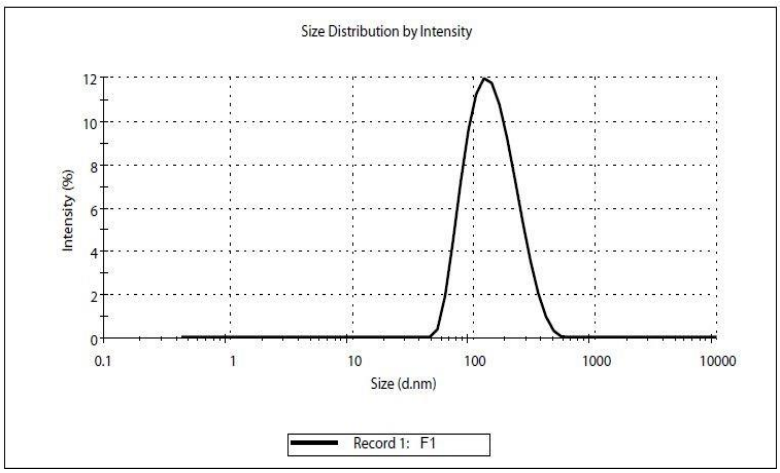

Fig. 8: Particle size of optimized astragalin-loaded polymeric nanoparticle

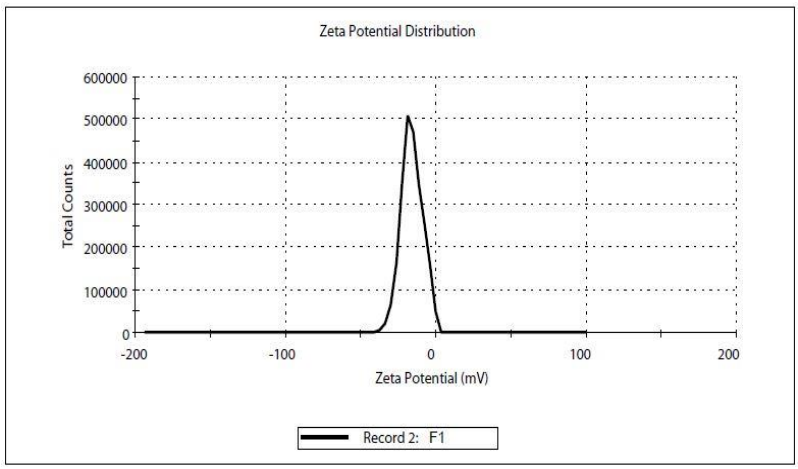

Fig. 9: Zeta potential of optimized astragalin-loaded polymeric nanoparticle

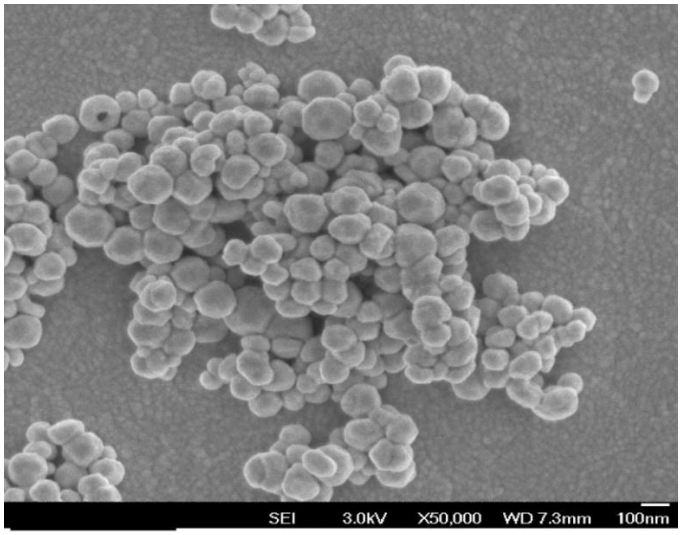

Fig. 10: SEM image of optimized astragalin-loaded polymeric nanoparticle

Differential scanning calorimetry (DSC) analysis

Differential scanning calorimetry (DSC) is a thermal analytical technique that measures the energy absorbed or emitted by a sample as a function of temperature [17]. The thermal behavior of astragalin was investigated by DSC. The pure astragalin shows a sharp endothermic peak that corresponds to the melting point at 202 °C. The Thermogram of PLA showed a sharp endothermic peak at 165 °C (fig. 11). The DSC thermogram of astragalin was compared with the DSC thermogram of the mixture of astragalin and polymer used in the formulation and there should be no interference in the peak of drug and polymer. The DSC of the mixture of drug sample and polymer was found to be within the specified range. Hence there is no interaction between the drug sample and the polymer likely to be used in the formulation and can be used in the formulation.

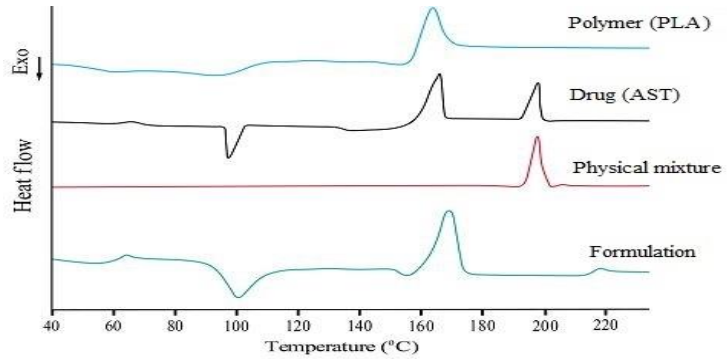

Fig. 11: DSC of astragalin, PLA, physical mixture, and nanoformulation

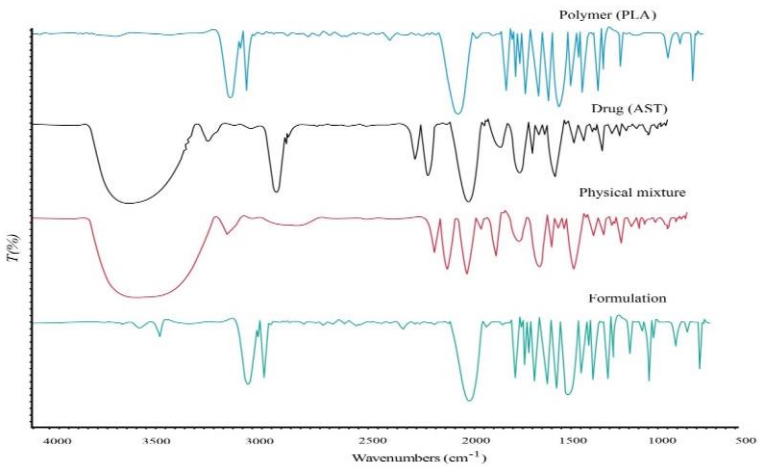

Fig. 12: FTIR of astragalin, PLA, physical mixture, and nanoformulation

Fourier transmission infrared spectroscopy (FTIR) analysis

FTIR analysis is used to study the interactions between astragalin and the polymer PLA used in the formulation. The infrared spectra of astragalin, the polymer used, their physical mixture, and the formulation of the same were shown in fig. 12. The IR of the mixture of drug sample and PLA were found to be within the specified range. Hence there is no interaction between the drug sample and the polymer likely to be used in the formulation and can be used in the formulation [18]. Astragalin procured their entire characteristic peak in the physical mixture. That is a significant peak 806-1653 were retained in the physical mixture. The frequency vibration of C=C stretching of AST at 1653 and 1613 cm^{-1} shifted to 1686 and 1628 cm^{-1}, respectively. The out-of-plane C–H bending at 806 cm^{-1}in AST shifted to 795 cm^{-1} in the complex. Other minor changes (shifting/intensity variation) were also observed in AST at 1362 cm^{-1} (in-plane OH bend), 1208 cm^{-1}(C–O stretching), 1508 and 1448 cm^{-1} (C–C stretching (in the ring)) based on FTIR spectra investigation no chemical interaction were observed between drug and polymer.

The *in vitro* drug release study

The most desirable feature of an anticancer formulation is the ability to remain stable at physiological pH while releasing their payloads at the tumor site [19]. Drug *in vitro* release tests were performed using the dialysis bag method. Astragalin-loaded PLA nanoparticles (5 mg) were added into a Phosphate Buffer, pH adjusted to 7.4, and were magnetically stirred for 32 h. The amount of astragalin released from the nanoparticles was monitored at 30, 60, 90, 120, 150, 180, 210, 240, and 270 min.

The results showed that astragalin was rapidly released in phosphate buffer solution, with a cumulative release rate of approximately 94% in 120 min. The astragalin-loaded PLA nanoparticles had a sustained-release effect and were released rapidly with a 65% cumulative release during the first 120 min and subsequent steady and slow release. Compared to AST, the AST-PLA-NPs demonstrated an obvious sustained-release effect *in vitro*.

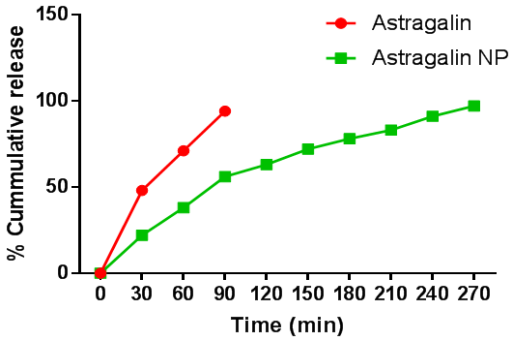

Fig. 13: Cumulative percentage drug release of pure drug astragalin and astragalin-loaded polymeric nanoparticles in PBS (pH 7.4)

Stability of astragalin-loaded polymeric nanoparticles

No significant difference was observed in Particle size, Zeta potential, Assay, and *in vitro* drug release for the formulation stored in 2-8 °C and 25 °C for 6 mo. Astragalin-loaded polymeric nanoparticles were found stable.

Table 5: Stability results

Storage condition		**25 °C/60% RH**		**2-8 °C**		
Time point	**Initial**	**3 Mo**	**6 Mo**	**1 Mo**	**3 Mo**	**6 Mo**
Description	Colloidal Dispersion	No Change	No Change	No Change	No Change	No Change
Particle Size (nm)	121±2.6	128±2.3	132±1.9	120±2.1	124±2.2	125±1.8
Zeta Potential (mV)	-25±1.4	-23±1.2	-22±1.1	-25±1.2	-25±1.1	-23±0.9
Assay	99%±0.9	98.50%±0.7	99.20%±0.6	100%±0.8	99%±0.5	99%±0.8
In vitro release at 210 min	94%±0.7	92%±0.5	95%±0.8	93%±0.9	95%±0.6	97%±0.7

Data represent mean±SD, n = 3

CONCLUSION

In this current research to develop better drug delivery systems, an attempt was made through an experimental design approach to optimize and formulate Astragalin-loaded polymeric nanoparticles. The central composite factorial design was used to analyze the effect of formulation variables on particle size, zeta potential, and encapsulation efficiency of the polymeric nanoparticles. The polynomial equations and response plots soundly justified the interrelationship between the dependent response and the independent variables. Polymer concentration, Stirring time and Aqueous organic phase ratio impacts the particle size, zeta potential, and encapsulation efficiency of polymeric nanoparticles.

The optimized formulation was prepared with a polymer concentration of 50 mg/ml, stirring time 60 min, aqueous to organic phase ratio of 5:1. The final formulation particle size is 121 nm, Zeta potential-25mV with an encapsulation efficiency of 89%. The stability studies conducted on optimized formulation establish the polymeric nano formulation's physical and chemical stability.

FUNDING

Nil

AUTHORS CONTRIBUTIONS

All authors have contributed equally.

CONFLICT OF INTERESTS

Declared none

REFERENCES

1. Newman DJ, Cragg GM. Natural products as sources of new drugs over the 30 years from 1981 to 2010. J Nat Prod. 2012;75(3):311-35. doi: 10.1021/np200906s, PMID 22316239.
2. Riaz A, Rasul A, Hussain G, Zahoor MK, Jabeen F, Subhani Z. Astragalin: A bioactive phytochemical with potential therapeutic activities. Adv Pharmacol Sci. 2018;2018:9794625. doi: 10.1155/2018/9794625, PMID 29853868.
3. Mehdi A, Al-Ani WMK, Raoof A. Isolation of astragalin from iraqi chenopodium album. Asian J Pharm Clin Res. 2018;11(12):530-5. doi: 10.22159/ajpcr.2018.v11i12.27958.
4. Kotani M, Matsumoto M, Fujita A, Higa S, Wang W, Suemura M. Persimmon leaf extract and astragalin inhibit the development of dermatitis and IgE elevation in NC/Nga mice. J Allergy Clin Immunol. 2000;106:159-66. doi: 10.1067/mai.2000.107194, PMID 10887319.
5. Bitis L, Kultur S, Melikoglu G, Ozsoy N, Can A. Flavonoids and antioxidant activity of rosa agrestis leaves. Nat Prod Res. 2010;24(6):580-9. doi: 10.1080/14786410903075507, PMID 20397108.
6. Kim YH, Choi YJ, Kang MK, Park SH, Antika LD, Lee EJ. Astragalin inhibits allergic inflammation and airway thickening in ovalbumin-challenged mice. J Agric Food Chem. 2017;65(4):836-45. doi: 10.1021/acs.jafc.6b05160, PMID 28064485.
7. Burmistrova O, Quintana J, Díaz JG, Estevez F. Astragalin heptaacetate-induced cell death in human leukemia cells is dependent on caspases and activates the MAPK

pathway. Cancer Lett. 2011;309(1):71-7. doi: 10.1016/j.canlet.2011.05.018, PMID 21658841.

8. Bainey KR, Armstrong PW. Clinical perspectives on reperfusion injury in acute myocardial infarction. Am Heart J. 2014;167(5):637-45. doi: 10.1016/j.ahj.2014.01.015, PMID 24766972.
9. Pathak S, Vyas SP, Pandey A. Development, characterization, and *in vitro* release kinetic studies of ibandronate loaded chitosan nanoparticles for effective management of osteoporosis. Int J Appl Pharm. 2021;13(6):120-5.
10. El-Assal MI, Samuel D. Optimization of rivastigmine chitosan nanoparticles for neurodegenerative Alzheimer; *in vitro* and ex vivo characterizations. Int J Pharm Pharm Sci. 2021;14(1):17-27. doi: 10.22159/ijpps.2022v14i1.43145.
11. Esfanjani AF, Seid Mahdi Jafari. Biopolymer nanoparticles and natural nanocarriers for nano-encapsulation of phenolic compounds. Colloids and Surfaces B: Biointerfaces; 2016. doi: 10.1016/j.colsurfb.2016.06.053.
12. Couvreur P, Dubernet C, Puisieux F. Controlled drug delivery with nanoparticles: current possibilities and future trends. Eur J Pharm Biopharm. 1995:2-13.
13. Kreuter J. Colloidal drug delivery systems. CRC Press; 1994.
14. Nah JW, Paek YW, Jeong YI, Kim DW, Cho CS, Kim SH. Clonazepam release from poly(DL-lactide-co-glycolide) nanoparticles prepared by dialysis method. Arch Pharm Res. 1998;21(4):418-22. doi: 10.1007/BF02974636, PMID 9875469.
15. Das J, Debbarma A, Lalhlenmawia. Formulation and *in vitro* evaluation of poly(d, l-lactide-co-glycolide) (plga) nanoparticles of ellagic acid and its effect on human breast cancer, mcf-7 cell line. Int J Curr Pharm Res. 2021;13(5):56-62.
16. Barhoum A, Garcia Betancourt ML, Rahier H, Assche GV. Physicochemical characterization of nanomaterials: polymorph, composition, wettability, and thermal stability. In: Emerging applications of nanoparticles and architecture nanostructures current prospects and future trends micro and Nanotechnologies. Acdemia Press; 2018. p. 255-78.
17. Koshy O, Subramanian L, Thomas S, Chapter 5. Differential scanning calorimetry in nanoscience and nanotechnology. In: Thomas S, Thomas Raju, Zachariah AK, Mishra RK, editors, Micro and nano technologies, thermal and rheological measurement techniques for nanomaterials characterization. Elsevier; 2017. p. 109-22.
18. Ma Y, Zheng Y, Liu K, Tian G, Tian Y, Xu L. Nanoparticles of poly(Lactide-Co-Glycolide)-d-a-tocopheryl polyethylene glycol 1000 succinate random copolymer for cancer treatment. Nanoscale Res Lett. 2010;5(7):1161-9. doi: 10.1007/s11671-010-9620-3, PMID 20596457.
19. Liu J, Huang Y, Kumar A, Tan A, Jin S, Mozhi A. pH-sensitive nano-systems for drug delivery in cancer therapy. Biotechnol Adv. 2014;32(4):693-710. doi: 10.1016/j.biotechadv.2013.11.009, PMID 24309541.